Efficient Estimation of the Human Circadian Phase via Kalman Filtering

Chukwuemeka O. Ike^{1,2}, John T. Wen^{1,2}, Meeko M.K. Oishi³, Lee K. Brown⁴, and A. Agung Julius^{1,2}

Abstract—Circadian rhythms play a vital role in maintaining a person's well-being but remain difficult to quantify accurately. Numerous approaches exist to measure these rhythms, but they often suffer from performance issues on the individual level. This work implements a Steady-State Kalman Filter as a method for estimating the circadian phase shifts from biometric signals. Our framework can automatically fit the filter's parameters to biometric data obtained for each individual, and we were able to consistently estimate the phase shift within 1 hour of melatonin estimates on 100% of all subjects in this study. The estimation method opens up the possibility of real-time control and assessment of the circadian system, as well as chronotherapeutic intervention.

Clinical relevance— This establishes a near real-time alternative to melatonin measurements for the estimation of circadian phase shifts, with potential applications in feedback circadian control and chronotherapeutics.

I. INTRODUCTION

Circadian rhythms are biological processes that follow an approximate 24-hour cycle and play a vital role in maintaining an individual's well-being. These rhythms include the sleep-wake cycle, core body temperature (CBT), and a host of hormonal production cycles, which work in concert to keep a person in sync with their external environment. Disruptions in the circadian system have been found to have numerous short- and long-term effects, ranging from low productivity and digestive issues, to diabetes and certain cancers [22, 12]. These findings have motivated research into the field of circadian rhythms estimation, with techniques being developed to assess and mitigate the effects of circadian disruption.

Circadian rhythms are known to be maintained by numerous peripheral oscillators, which are all kept synchronized by the principal clock known as the suprachiasmatic nuclei (SCN) located in the brain. Due to its physical location, the SCN is inaccessible for measurements, so work in the field has focused on the use of downstream signals that are driven by the circadian clock as proxies for the true circadian state. The most widely used signals include melatonin concentration in blood, saliva, or urine; CBT, activity levels, skin temperature, and heart rate [1, 4, 17].

1,2Chukwuemeka O. Ike, John T. Wen, and A. Agung Julius are with the Lighting Enabled Systems and Applications (LESA) Engineering Research Center, Troy, NY, USA; and the Department of Electrical, Computer, and Systems Engineering, Rensselaer Polytechnic Institute, Troy, NY, USA. {ikec,wenj,juliua2}@rpi.edu

³Meeko M.K. Oishi is with the Department of Electrical and Computer Engineering, University of New Mexico, Albuquerque, NM, USA.

⁴Lee K. Brown is with the Department of Internal Medicine, University of New Mexico, Albuquerque, NM, USA.

Many of these signals serve as both inputs and outputs of the circadian system, and are also open to numerous external disturbances - for example, exercise directly affects heart rate. As such, they are prone to masking factors that further compound the task of circadian estimation [9]. Melatonin possesses a relatively strong resistance to masking, and is thus the current clinical standard for circadian phase estimation. Particularly, research has used the time at which melatonin concentrations reach a specified threshold in low light - the dim light melatonin onset (DLMO) - as a circadian phase marker since it was first proposed by Lewy et al. in [16]. However, melatonin measurements are burdensome and difficult outside of clinical conditions, thus preventing the study of individuals in their natural environment. Moreover, the melatonin values only become available after samples are processed in a lab, eliminating the method's usefulness in near real-time applications. For estimates of the circadian state to be useful in applications like feedback control of the circadian system and chronotherapeutics, a continuous estimation method is still needed [8].

Multiple model-based and model-free approaches exist that use more accessible data streams [6, 13, 7]. However, many of these methods are accurate on the population average, but performance tends to suffer on the individual level where it is most needed [21]. Moreover, different data streams possess different characteristics, leading to further difficulties in employing the same single-input algorithm across data types.

There have also been methods of estimating circadian characteristics using techniques borrowed from signal processing for approximately periodic time series. These include wavelet analysis methods which identify the period and amplitude information of the rhythms localized in the time-domain [15, 14], Fourier analysis, and auto-regressive modeling [5]. Many of these methods estimate the circadian system's parameters (often period and/or amplitude), after which the parameters can be used in a subsequent estimation technique. Woelders et al. used an estimated circadian period in the Kronauer model to achieve improved performance [24].

In this paper, we demonstrate the use of a steady-state Kalman filter in continuously estimating the human circadian phase in entrained conditions on an individualized basis. In our previous work, we proposed the use of a linear state observer for the same task [10]. We compared the method against the gold standard DLMO values obtained during a clinical study and achieved an average estimation error of 1.5 hours across all subjects. We also compared the method against the adaptive notch filter (ANF) from [26] and found

that it was a superior algorithm with a fraction of the ANF's computational cost. In this paper, we instead use a Kalman filter and show that the method is more consistently accurate than the observer-based filter (OBF) from [10], while providing the same advantages of the OBF over DLMO and the ANF.

To address the problem of individualization, we implement a method that tunes the parameters of the filter based on the specific individual's data provided. In [10], we parameterized the filter optimization with the observer gain vector L, and directly searched for each of the vector's elements. In this paper, we instead parameterize the optimization with the filter's covariance parameters, and we found that doing so improved the accuracy and precision of our phase shift estimates. The tuning method is also able to learn the characteristics of the specific data stream used (actigraphy, light exposure, CBT, etc.). The resulting Kalman filter estimator achieved phase shift estimates within ± 1 hour of the DLMO-based estimates for 100% of the subjects in the study.

II. METHODS

A. Experimental setup

1) Data Collection: The same dataset was used in the validation of the methods in [26] and [10]. We collected the actigraphy data of eight healthy young adults (5 female and 3 male) aged between 18 and 34 y (25.8 \pm 6.6 y). The data was collected over an 8-month period, but the filter was tested on data over a 2-week period to minimize the role that weather and climate played. This is because the length of the day and natural light exposure can be assumed to be largely the same from one week to the next. Actigraphy data was recorded with an ActiGraph GT3X+ Monitor (Pensacola, FL) worn on each subject's non-dominant wrist. The device took readings at 1-minute intervals over the 2 weeks, providing near real-time data on subject behavior.

Melatonin measurements were taken on the 7th and 14th days via saliva swabs collected at 30-minute intervals with Salimetrics SalivaBio Oral Swabs (State College, PA). The samples were taken with subjects in dim lighting and in a supine position, starting approximately 5 hours before and ending 30 minutes after the average bedtime. Participants accumulated saliva for 2 minutes, after which they stored the samples at -20°C. For analysis, the samples were thawed and centrifuged for 10 minutes at 2500 rpm.

All participants gave their informed written consent, and the experiments followed the principles in the Declaration of Helsinki from the World Medical Association. The experiments were monitored by the University of New Mexico (UNM) Health Sciences Center Human Research Protections office and approved by the UNM Institutional Review Board (IRB). The study's IRB number is 14-002.

2) Simulation Environment: All numerical experiments were done using MATLAB R2021a on a Dell workstation equipped with an Intel Core i7-3770 3.40GHz processor and 16GB of RAM.

B. Problem Formulation

In our work, we assume that the nominal noiseless biometric signal (e.g., actigraphy) is periodic and can thus be approximated using a Fourier series. This periodic signal can then be represented as a sum of K harmonics and a bias term, in the form

$$y_k = d + \sum_{i=1}^K a_i \sin(i\omega^* k + \phi_i), \tag{1}$$

where y_k is the signal value at time-step k, ω^* is the fundamental frequency of the signal which we assume to be fixed at $\frac{2\pi}{24} rad/h$ (corresponding to a 24 hour period), d is the constant bias term; and a_i and ϕ_i are the amplitude and phase offset of the i-th harmonic, respectively. The sinusoidal components of this signal can then be assumed to be the outputs of K harmonically related linear oscillators represented by the autonomous discrete-time system

$$x_k = Ax_{k-1}, \qquad y_k = Cx_k, \tag{2}$$

where x_k and y_k are the system state and output at time-step k, respectively; A is the state dynamics model, and C is the observation model. We choose A and C to be

$$A = \begin{bmatrix} A_1 & 0 & \dots & 0 & 0 \\ 0 & A_2 & \dots & 0 & 0 \\ \vdots & \vdots & \ddots & \vdots & \vdots \\ 0 & 0 & \dots & A_K & 0 \\ 0 & 0 & \dots & 0 & 0 \end{bmatrix}, \quad C = \begin{bmatrix} C_1 & C_2 & \dots & C_K & 1 \end{bmatrix}$$

with submatrices

$$A_i = \begin{bmatrix} 0 & 1 \\ -(i\omega^*)^2 & 0 \end{bmatrix}, \quad C_i = \begin{bmatrix} 0 & \frac{2}{i\omega^*} \end{bmatrix}, \quad i \in \{1, \dots, K\},$$

which represents our view of the biometric data y_k as the sum of K harmonics.

We design a Kalman filter (KF) to simultaneously estimate the states of each of these oscillators. In practice, the parameters of the biometric signal are time-varying, so the KF tracks the deviation of each from the nominal values produced by the oscillators.

Remark: Note that the model above is <u>not</u> a model of the biochemical and/or regulatory processes that constitute the circadian rhythms, which is typically nonlinear. Our goal is not to estimate the states of such processes. Rather, we aim to estimate the phase <u>shift</u> in a noisy biometric signal, which is nominally periodic.

C. Kalman Filtering

The Kalman filter is a state estimation algorithm that accounts for the uncertainty in both the system's dynamics and in output measurements. It is best suited to a discrete-time system given by

$$x_k = Ax_{k-1} + w_k, \qquad y_k = Cx_k + v_k,$$

which is the same system as in Equation 2 with additional terms $w_k \sim \mathcal{N}(0,Q)$ as the process noise drawn from a zero-mean multivariate normal distribution with covariance $Q \in$

 $\mathbb{R}^{n \times n}$, n the system's dimension, and $v_k \sim \mathcal{N}(0,R)$ as the observation noise drawn from a zero-mean normal distribution with covariance $R \in \mathbb{R}^+$. The initial state and the noise vectors at each step are also assumed to be mutually independent.

The recursive version of the filter involves a prediction step where estimates are predicted in the absence of measurements, and an update step where the predictions are corrected based on the latest measurement. This process repeats until the estimate covariance and the Kalman gain reach a steady-state. However, this recursion can be replaced with the use of a steady-state version of the filter conditioned on the following assumptions [20]:

- 1) The pair (A,C) is detectable
- 2) The pair (A, Q_f^T) is stabilizable, where $Q = Q_f Q_f^T$
- 3) Q is positive semi-definite
- 4) R is positive definite.

To use the steady-state version of the Kalman filter, we first solve the algebraic Riccati equation (ARE)

$$\hat{P} = A\hat{P}A^T + Q - A\hat{P}C^T(C\hat{P}C^T + R)^{-1}C\hat{P}A^T$$

for \hat{P} , where \hat{P} is the estimate covariance, Q and R are the covariance parameters described above, and A and C are from Equation 2. The solution of this equation is then used in calculating the steady-state Kalman gain

$$L = A\hat{P}C^T(C\hat{P}C^T + R)^{-1}.$$

We use this gain in the filter updates, and the filter functions similarly to a time-invariant observer with update equations given by

$$\hat{x}_k = A\hat{x}_{k-1} + L(y_{k-1} - \hat{y}_{k-1})$$

$$\hat{y}_k = C\hat{x}_k,$$
(3)

where \hat{x} is the filter's state estimate, and \hat{y} is the output estimate whose Fourier transform we attempt to match with that of the input signal. We use this steady-state KF to estimate the circadian phase in our work, as it runs significantly faster than the recursive version, with near-identical performance.

D. Filter Optimization

To account for variations in circadian dynamics across people, we tune the filter's covariance parameters Q and R for each individual using the cost function from [26] detailed below.

$$F(Y(\omega), \hat{Y}(\omega)) = J_{harmo} + J_{noise}, \tag{4}$$

with

$$J_{harmo} = \int_0^{\delta \omega} [Y(\omega) - \hat{Y}(\omega)]^2 d\omega + \sum_{n=1}^K \int_{n\omega^* - \delta \omega}^{n\omega^* + \delta \omega} [Y(\omega) - \hat{Y}(\omega)]^2 d\omega$$

and

$$J_{noise} = \sum_{n=0}^{K-1} \int_{n\omega^* + \delta\omega}^{(n+1)\omega^* - \delta\omega} \hat{Y}(\omega)^2 d\omega + \int_{K\omega^* + \delta\omega}^{+\infty} \hat{Y}(\omega)^2 d\omega,$$

where J_{harmo} represents the square error around each component and the bias term, J_{noise} is the filtered output outside the desired components, K is the filter order being used, and $Y(\omega)$ and $\hat{Y}(\omega)$ are the Fourier transforms of the input biometric signal and the filter output, respectively. $\delta\omega$ represents the assumed bandwidth of the harmonics, which is set at 0.06786 rad/hour, chosen based on the phase dynamics for light intensities less than 1000 lux as measured during the experiments[26, 11].

The optimization variables are the covariance parameters Q and R from above, and we optimize using the evolutionary strategy [18] detailed in algorithm 1 on the cost function (4). The optimization starts with μ members of the population, and at each iteration, we create λ offspring using ρ members each, run the filter with each new member, calculate the costs, then remove the members with the λ highest costs. Each offspring is generated by taking the arithmetic mean of ρ random members of the population, making the evolution more transparent compared to the standard Genetic Algorithm.

This process is repeated for a specified number of iterations, after which the best parameters can be used on the subject's biometric data. We found that in contrast to [10] where we parameterized the optimization with the observer gains L, the parameterization using Q and R provided more consistently accurate results.

Each population member is a pair of a random matrix Q_f and a random positive real number R. To yield a symmetric positive definite matrix for the process noise covariance, we take

$$Q = Q_f \cdot Q_f^T$$
.

E. Filter-based Circadian Phase Shift Estimation

Once the filter has been tuned, we can use it in estimating the phase shift between any two days. We take the estimated circadian phase at a given time-step k to be the argument of the first harmonic term as represented by the first two state estimates of the KF

$$\hat{\phi}_{1,k} \triangleq -\arctan\left(\frac{\hat{x}_{2,k}}{\boldsymbol{\omega}^* \cdot \hat{x}_{1,k}}\right).$$

This is in line with the assumption that the fundamental harmonic of the input signal is representative of the person's circadian state. We define the circadian phase on a given day to be the average value of $\hat{\phi}_{1,k}$ on that day. Thus, to estimate the circadian phase shift between the 7th day and the 14th day, we compare the average phase on those days. A positive value here represents a phase delay, suggesting that circadian oscillation occurred later in time on the 14th day than it did on the 7th. This is analogous to the standard of measuring phase shift with melatonin, where the phase marker for a given day is compared with that of another to yield the phase shift.

Algorithm 1: Covariance Optimization

Input: max_iterations, y, μ , λ , ρ

Initialize:

```
Create initial populations Q_{pop} and R_{pop}
Create state space matrices A and C
for i = 1, \dots, \mu do
     Q \longleftarrow Q_{pop}(i) \cdot Q_{pop}(i)^T
     \tilde{R} \longleftarrow R_{pop}(i)
\hat{P} \longleftarrow ARE(A,C,R,Q)
     if \hat{P} exists then
           L \longleftarrow getKalmanGain(A, C, \hat{P}, R)
           \hat{\mathbf{y}} \leftarrow runKalmanFilter(A, C, L, \mathbf{y})
           Cost(i) \longleftarrow F(Y(\boldsymbol{\omega}), \hat{Y}(\boldsymbol{\omega}))
     else
           Cost(i) \leftarrow int\_max
     end
end
Iteratively improve population:
for i = 1, ..., max\_iterations do
     for j = \mu + 1, ..., \mu + \lambda do
           Q_{combo}, R_{combo} \longleftarrow \rho random members
           Q_{pop}(j) \longleftarrow mean(Q_{combo})
           R_{pop}(j) \longleftarrow mean(R_{combo})
           Q \longleftarrow Q_{pop}(j) \cdot Q_{pop}(j)^T
           R \longleftarrow R_{pop}(j)
           \hat{P} \longleftarrow ARE(A, C, R, Q)
           if \hat{P} exists then
                 L \longleftarrow getKalmanGain(A, C, \hat{P}, R)
                 \hat{y} \leftarrow runKalmanFilter(A, C, L, y)
                 Cost(j) \longleftarrow F(Y(\boldsymbol{\omega}), \hat{Y}(\boldsymbol{\omega}))
           else
                Cost(j) \leftarrow int\_max
           end
     end
     Remove \lambda highest costs and corresponding
       population members
end
Result: Optimal parameters Q_{opt} and R_{opt}
```

III. RESULTS

In this section, we compare the results of running 100 independent optimizations each of the KF and the OBF. From previous testing of the OBF, we found that the third order version of the filter consistently outperformed other versions [10], so we compare the KF to the third order OBF. The number of optimization variables for the KF increases nonlinearly with the filter order, since the matrix Q_f has $(2K+1)^2$ entries, where K is the filter order. Because of this, optimization beyond the first order requires a larger population size and consequently, longer optimization time. Moreover, this increase in filter order did not yield a significant increase in the filter's performance, so we opted to use the first order KF in our work. The results presented are thus a comparison between the third order OBF and the first order

KF - the best performing versions of each filter.

A. Phase Shift Estimation Accuracy

The accuracy of the phase shift estimates serves as the most important quantifier of the algorithm's usefulness. In Figure 1, we compare the OBF and KF's phase shift estimates with the DLMO-based estimates obtained for each subject. There are up to 3 DLMO values for each subject, as we calculated it with the methods from [16], [2], and [23], which all choose the thresholds slightly differently. [16] chooses a fixed threshold to use for all subjects. [2] sets each subject's threshold as twice the mean of that person's first three low daytime values. [23] takes the mean of the subject's first three low values and adds 2 standard deviations. For any given subject, we can thus have up to 3 distinct DLMO estimates as seen in Figure 1. None of the three methods yielded DLMO values for subjects 5 and 9, so we exclude those subjects in the results reported.

We see that the KF provides more consistent estimates that are closer to the DLMO-based estimates than the OBF across all subjects. To further evaluate the comparative level of agreement of the KF's estimates with the DLMO-based ones, we performed a right-tailed t-test on the absolute deviations of both filters' estimates from the average DLMO values. More specifically, we tested the null hypothesis that the filters' deviations were the same versus the alternative that the OBF's deviations were greater. The results are displayed numerically in Table I and graphically in Figure 2. In 4 of the 6 subjects, we found that the KF outperformed the OBF at the 5% significance level. In subjects 8 and 10, the required significance was not met. However, after testing the opposite alternative hypothesis, we found that the KF's deviations were not higher than the OBF's, implying that in these cases, the KF performs on par with the OBF and not worse. These results help confirm that the Kalman filter provides a solid and consistent improvement over the OBF in entrained circadian conditions.

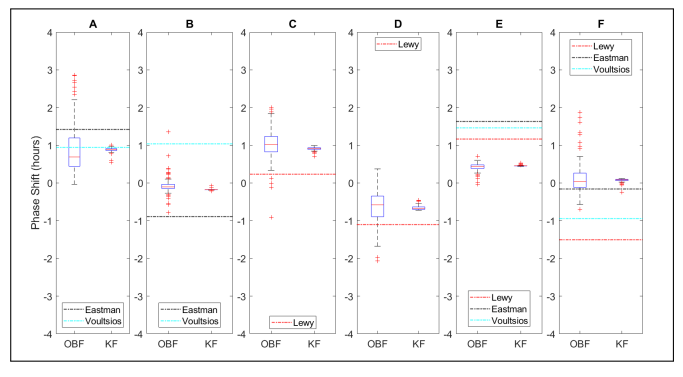


Fig. 1: Phase Shift Estimates for Subjects (A) 3, (B) 4, (C) 6, (D) 7, (E) 8, and (F) 10. Note: Box-plot variations are due to the random initialization of the filters' parameters for each optimization.

TABLE I: Average Absolute Deviation (in minutes) from the Average DLMO Values By Subject.

¹Hypothesis test results - 0 indicates mean deviations are statistically same, 1 indicates OBF deviations are higher.

²Significance level - smaller values cast doubt on validity of null hypothesis. The chosen threshold here was 5.0×10^{-2} .

	OBF		KF (this paper)			
Subject	Mean (± Std)	% within 1 hr	Mean (± Std)	% within 1 hr	h ¹	p^2
3	38.6 (±20.6)	91	17.9 (±3.76)	100	1	3.787×10^{-19}
4	13.1 (±10.5)	99	15.0 (±0.742)	100	0	9.688×10^{-1}
6	49.9 (±21.2)	74	40.5 (±2.30)	100	1	8.841×10^{-6}
7	40.3 (±61.0)	83	26.5 (±3.35)	100	1	1.207×10^{-2}
8	60.0 (±6.54)	58	57.9 (±0.757)	100	1	8.038×10^{-4}
10	60.4 (±26.7)	61	56.6 (±2.66)	100	0	7.433×10^{-2}

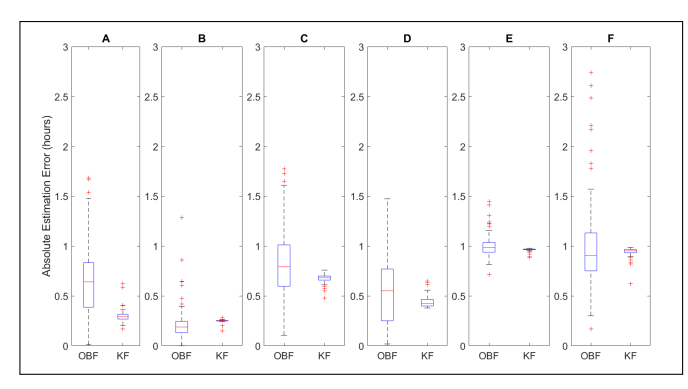


Fig. 2: Absolute Deviation from Average DLMO-based estimates for Subjects (A) 3, (B) 4, (C) 6, (D) 7, (E) 8, and (F) 10. Note: Box-plot variations are due to the random initialization of the filters' parameters for each optimization.

B. Optimization Runtimes

The efficiency of algorithms proposed for continuous estimation of the circadian phase is an important performance metric, as the ability to deploy these methods on computationally constrained devices has a direct effect on their potential usefulness. To this end, we evaluate the algorithm's efficiency using the optimization runtimes and compare them to the OBF's. Across all subjects, we found the average OBF runtime to be 26.3 seconds, while the average KF runtime was 29.5 seconds. Figure 3 visualizes this, and we see that the KF runs nearly as fast as the OBF. We thus get a slight slowdown by using the KF, but with the advantage of increasing the accuracy and consistency of the estimated phase shifts as seen in the previous section.

IV. CONCLUSION

In this paper, we described a method for continuous circadian phase estimation using a Kalman filter with easily accessible physiological signals. By assuming a form on the circadian signals and carefully parameterizing the filter optimization, we were able to tune a Kalman filter to isolate the fundamental harmonic of the signals, and to subsequently estimate the change in phase using the filter's output. The estimator consistently achieved phase shift estimates within 1 hour of the average DLMO-based estimates on 100% of

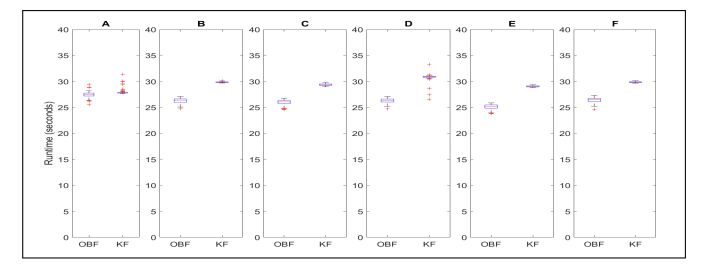


Fig. 3: Runtimes for Subjects (A) 3, (B) 4, (C) 6, (D) 7, (E) 8, and (F) 10. Note: Box-plot variations are due to the random initialization of the filters' parameters for each optimization.

the subjects studied, suggesting that the method is potentially useful as a low-burden alternative to DLMO in entrained settings.

The ability to assess the circadian phase in real-time using the method proposed here opens up the ability to incorporate the measurements both in methods of controlling the circadian system, and in general studies of circadian rhythms. Current methods for circadian control tend to rely on open-loop approaches to guiding the circadian system to a goal state [27, 25, 19, 3]. Real-time estimates of the circadian state have the potential to improve the design and subsequent efficacy of control methods.

One potential avenue of future research is the incorporation of multiple signals to improve estimation accuracy. It has been shown in multiple instances that the combination of external stimuli - often light - and biometric signals can often improve the performance of the algorithm used [21, 13]. We intend to explore the possibility of a multi-input KF estimator and evaluate how the method performs in comparison to DLMO.

ACKNOWLEDGMENTS

This work was primarily supported by the National Science Foundation (NSF) through Grant DMS-2037357 and the Smart Lighting Engineering Research Center (EEC-0812056), the Army Research Office through Grant W911NF-17-1-0562 and W911NF-22-10039, and New York State under NYSTAR contract C130145. The authors would like to thank Dr. Jiawei Yin for his contribution to the initial portion of this research as part of his doctoral research and to the staff of the University of New Mexico Hospital Sleep Disorders Center who carried

out the DLMO procedures: Steven Lopez, Alex Valdez, Cielo Ortiz, and Ryan Valdez.

REFERENCES

- [1] Clark Bowman et al. "A method for characterizing daily physiology from widely used wearables". In: *Cell reports methods* 1.4 (2021), p. 100058.
- [2] Helen J Burgess and Charmane I Eastman. "The dim light melatonin onset following fixed and free sleep schedules". In: *Journal of sleep research* 14.3 (2005), pp. 229–237.
- [3] Samuel Christensen et al. "Optimal adjustment of the human circadian clock in the real world". In: *PLOS Computational Biology* 16.12 (2020), e1008445.
- [4] André Dittmar et al. "A non invasive wearable sensor for the measurement of brain temperature". In: 2006 International Conference of the IEEE Engineering in Medicine and Biology Society. IEEE. 2006, pp. 900– 902.
- [5] Harold B Dowse. "Maximum entropy spectral analysis for circadian rhythms: theory, history and practice". In: *Journal of circadian rhythms* 11.1 (2013), pp. 1–9.
- [6] Daniel B Forger, Megan E Jewett, and Richard E Kronauer. "A simpler model of the human circadian pacemaker". In: *Journal of biological rhythms* 14.6 (1999), pp. 533–538.
- [7] Enrique A Gil, Xavier L Aubert, and Domien GM Beersma. "Ambulatory estimation of human circadian phase using models of varying complexity based on non-invasive signal modalities". In: 2014 36th Annual International Conference of the IEEE Engineering in Medicine and Biology Society. IEEE. 2014, pp. 2278– 2281.
- [8] Joseph D Gleason et al. "A novel smart lighting clinical testbed". In: 2017 39th Annual International Conference of the IEEE Engineering in Medicine and Biology Society (EMBC). IEEE. 2017, pp. 4317–4320.
- [9] Kevin M Hannay and Jennette P Moreno. "Integrating wearable data into circadian models". In: *Current Opinion in Systems Biology* 22 (2020), pp. 32–38.
- [10] Chukwuemeka O Ike et al. "Fast Tuning of Observerbased Circadian Phase Estimator Using Biometric Data". In: *Heliyon* (2022), e12500.
- [11] A Agung Julius, Jiawei Yin, and John T Wen. "Time optimal entrainment control for circadian rhythm". In: *PloS one* 14.12 (2019), e0225988.
- [12] Anders Knutsson. "Health disorders of shift workers". In: *Occupational medicine* 53.2 (2003), pp. 103–108.
- [13] Vitaliy Kolodyazhniy et al. "An improved method for estimating human circadian phase derived from multichannel ambulatory monitoring and artificial neural networks". In: *Chronobiology International* 29.8 (2012), pp. 1078–1097.
- [14] Tanya L Leise. "Wavelet analysis of circadian and ultradian behavioral rhythms". In: *Journal of circadian rhythms* 11.1 (2013), pp. 1–9.

- [15] Tanya L Leise and Mary E Harrington. "Wavelet-based time series analysis of circadian rhythms". In: *Journal of biological rhythms* 26.5 (2011), pp. 454–463.
- [16] Alfred J Lewy and Robert L Sack. "The dim light melatonin onset as a marker for orcadian phase position". In: *Chronobiology international* 6.1 (1989), pp. 93–102.
- [17] Hazuki Masuda et al. "The estimation of circadian rhythm using smart wear". In: 2020 42nd Annual International Conference of the IEEE Engineering in Medicine & Biology Society (EMBC). IEEE. 2020, pp. 4239–4242.
- [18] E Ruffio et al. "Tutorial 2: Zero-order optimization algorithms". In: *Eurotherm School METTI* (2011).
- [19] Kirill Serkh and Daniel B Forger. "Optimal schedules of light exposure for rapidly correcting circadian misalignment". In: *PLoS computational biology* 10.4 (2014), e1003523.
- [20] Robert F Stengel. *Optimal control and estimation*. Courier Corporation, 1994.
- [21] Julia E Stone et al. "Computational approaches for individual circadian phase prediction in field settings". In: Current Opinion in Systems Biology 22 (2020), pp. 39–51.
- [22] Martha Hotz Vitaterna, Joseph S Takahashi, and Fred W Turek. "Overview of circadian rhythms". In: Alcohol Research & Health 25.2 (2001), p. 85.
- [23] Athena Voultsios, David J Kennaway, and Drew Dawson. "Salivary melatonin as a circadian phase marker: validation and comparison to plasma melatonin". In: *Journal of biological rhythms* 12.5 (1997), pp. 457–466.
- [24] Tom Woelders et al. "Daily light exposure patterns reveal phase and period of the human circadian clock". In: *Journal of biological rhythms* 32.3 (2017), pp. 274–286.
- [25] Jiawei Yin, A Agung Julius, and John T Wen. "Optimization of light exposure and sleep schedule for circadian rhythm entrainment". In: *Plos one* 16.6 (2021), e0251478.
- [26] Jiawei Yin et al. "Actigraphy-based parameter tuning process for adaptive notch filter and circadian phase shift estimation". In: *Chronobiology International* 37.11 (2020), pp. 1552–1564.
- [27] Jiaxiang Zhang, John T Wen, and Agung Julius. "Optimal circadian rhythm control with light input for rapid entrainment and improved vigilance". In: 2012 IEEE 51st IEEE Conference on Decision and Control (CDC). IEEE. 2012, pp. 3007–3012.